COGNITIVE NEUROSCIENCE

Shared neural representations and temporal segmentation of political content predict ideological similarity

Daantje de Bruin[1], Jeroen M. van Baar[1,2], Pedro L. Rodríguez[3,4], Oriel FeldmanHall[1,5]*

Despite receiving the same sensory input, opposing partisans often interpret political content in disparate ways. Jointly analyzing controlled and naturalistic functional magnetic resonance imaging data, we uncover the neurobiological mechanisms explaining how these divergent political viewpoints arise. Individuals who share an ideology have more similar neural representations of political words, experience greater neural synchrony during naturalistic political content, and temporally segment real-world information into the same meaningful units. In the striatum and amygdala, increasing intersubject similarity in neural representations of political concepts during a word reading task predicts enhanced synchronization of blood oxygen level–dependent time courses when viewing real-time, inflammatory political videos, revealing that polarization can arise from differences in the brain's affective valuations of political concepts. Together, this research shows that political ideology is shaped by semantic representations of political concepts processed in an environment free of any polarizing agenda and that these representations bias how real-world political information is construed into a polarized perspective.

INTRODUCTION

Following the 2020 U.S. Presidential election, the country appeared divided into two camps of tens of millions of partisans, each claiming to have won the Presidency. This momentary political impasse illustrates the widespread and destructive nature of polarized politics. Although political polarization is a growing problem, we know little about the neurobiological mechanisms that underpin it (*1*). One account argues that polarization manifests because political camps consume different sources of information through selective news outlets and curated social media accounts (*1*–*10*). If true, then exposure to alternative political perspectives should be able to disrupt political echo chambers and mitigate polarization. Recent research, however, suggests that exposure to an opposing political perspective only fuels a greater entrenchment of one's political beliefs (*11*). Another, complementary explanation holds that different beliefs can bias the interpretation of the same event (*12*), such that opposing groups of partisans may, for example, both believe that a single news broadcast was biased against their side (*13*). Polarization may thus arise as the brain processes incoming information: Individuals who hold opposing political beliefs construe the same information into a polarized perspective at the moment of perception (*13*–*18*).

Here, we evaluate the hypothesis that like-minded partisans share the same interpretation of events because they represent—and therefore structure their experience of—political content in the same way. To assess shared interpretation, we examine the level of neural synchrony (i.e., coordinated brain responses) among subjects exposed to the same information (*19*–*22*). Neural synchrony is an implicit corollary of shared processing that tracks mental coupling in real time. Recent research suggests that political allies exhibit synchronized neural dynamics when consuming real-world political content, such as political news coverage (*17*, *18*). Merely observing a synchronized neural fingerprint between individuals, however, leaves unanswered what is driving this synchronized response. In this research, we assess whether shared semantic representations of political concepts predict how people structure and experience dynamic, real-world political content, which, in turn, biases their political ideology.

Prior work shows that Republicans and Democrats differ in their semantic representations of politically charged concepts (*23*), which, in turn, correlate with political attitudes (*24*). These partisan semantic representations, potentially shaped by the consumption of different media sources, are influenced by the emotions evoked by political concepts (*25*–*28*) and the way in which political concepts are encoded into semantic memory (*24*, *29*). The effect of emotion on semantic representation is known to be especially salient when concepts are abstract (*24*–*26*, *29*), and in the political sphere, where many words do not have concrete or tangible meaning (e.g., *freedom*, *American*), this means that emotion is likely to play an outsized role in shaping semantic representations. For instance, the word *abortion* may conjure up a set of concepts and emotions that all converge on a similar experience among individuals who share a political affiliation [e.g., conservatives might associate the word *abortion* with *right to life*, *murder*, *personhood*, etc., while liberals might associate it with *right to choose*, *women's rights*, *personal autonomy*, etc.; (*30*)]. Neurally, this would be reflected by conservatives sharing one pattern of neural activity when processing the word *abortion* and liberals exhibiting a different neural pattern.

Because neural activity patterns store information about the world, how the brain represents this information is considered a metric for how that information is interpreted and used to steer behavior and attitudes (*31*, *32*). For example, semantic representations may bias downstream cognitive processes (*17*, *24*, *33*). If political

[1]Department of Cognitive, Linguistic, Psychological Sciences, Brown University, Providence, RI, USA. [2]Trimbos Institute, Netherlands Institute of Mental Health and Addiction, Utrecht, Netherlands. [3]Center for Data Science, New York University, New York, NY, USA. [4]International Faculty, Instituto de Estudios Superiores de Administración, Caracas, Venezuela. [5]Carney Institute for Brain Science, Brown University, Providence, RI, USA.
*Corresponding author. Email: oriel.feldmanhall@brown.edu

concepts are represented—and thus interpreted—in similar ways depending on a shared political affiliation, then we can also test whether these shared representations predict similar polarized interpretations of more naturalistic content.

When people are bombarded with a continuous stream of incoming information, one way in which individuals impose structure and meaning onto their unfolding subjective experience is by spontaneously segmenting this information into discrete narrative events or "scenes" (*34*, *35*). Recent work on temporal event segmentation shows that as the brain's perceptual system processes incoming information, segmented events are accompanied by relatively stable patterns of temporally reoccurring neural activity called neural states (*36*) that covary with discrete physiological and psychological states believed to reflect subjective engagement and emotional appraisal (*36*–*38*). From a political perspective, sharing a common temporal structure of neural patterns when consuming naturalistic political content might predict a shared ideological perspective. If true, then this would allow us to test whether chunking naturalistic information (e.g., a news broadcast) into the same meaningful units (*39*) also biases political polarization, providing an additional mechanism for why some people come to interpret the same content in two very different ways.

To assess whether political concepts are represented in a similar way by like-minded partisans, and whether these representations influence ongoing political information processing, we extract individual brain responses both during a controlled, contextless word reading task that may not necessarily lead to polarized interpretations and during a naturalistic viewing task where polarization is often spontaneously ignited (e.g., political debates and news coverage). We leverage a combination of imaging techniques, including representational similarity analysis [RSA; (*40*)] neural state segmentation (*35*, *36*), and blood oxygen level–dependent (BOLD) time series analyses, and then apply neural synchrony metrics (*41*, *42*) that correlate similarity of activity patterns and neural states between every pair of subjects. This allows us to test whether a shared understanding between political allies—construed at the level of either single words devoid of context or a barrage of audio-visual stimuli that is highly contextualized—relies on intersubject similarity at the representational level of processing.

Given the importance of emotion in both the representation and valuation of abstract concepts and politics in general (*27*, *28*, *43*, *44*), we posit that brain regions involved in encoding value and emotional content (*45*–*49*)—for example, the striatum and amygdala—play a role in generating a shared polarized perspective (*18*, *50*–*55*). In addition, as prior work demonstrates that shared understanding critically relies on the ability to take the perspective of another, we expect that regions involved in mentalizing—which include the dorsomedial prefrontal cortex (dmPFC) and temporoparietal junction [TPJ; (*12*, *56*–*59*)]—should reflect coordinated brain responses among copartisans. In short, reflecting the inherent richness of both political polarization and naturalistic neuroimaging experiments (*60*), we anticipate a neural model of polarization that includes regions involved in affective valuation and mentalizing.

Through targeted online and field recruiting (N = 360), we invited 44 participants (equally split among liberals and conservatives) to participate in a study on political cognition (Fig. 1). While undergoing functional magnetic resonance imaging (fMRI), participants first completed a word reading task where they were presented with single words (e.g., *immigration*, *abortion*) and asked to determine whether the word was political or nonpolitical (indicated via a button press). Participants then completed a video watching task in the scanner, including a neutrally worded news clip on abortion and a heated 2016 Vice-Presidential Debate on police brutality and immigration. We used data collected during these tasks to investigate the relationships between political ideology, the representation of political concepts, and the synchronization of neural states.

RESULTS

The processing of political concepts predicts political ideology

We began by testing whether distinct representations of political words predict partisans on the opposite sides of the political aisle. We used a behavioral measure—the spatial arrangement task (*61*) where participants are instructed to place each word (e.g., *abortion*, *religion*, *gang*, *welfare*, etc.) in a two-dimensional space based on their semantic similarity (Fig. 1D). The task included 30 political words that fell into conceptually distinct political categories, including "American," "police," "immigration," and "abortion" (see the Supplementary Materials for full list and more details on the choice of words). For each participant, we computed the Euclidean distance between each word and every other word, resulting in a participant-specific representational dissimilarity matrix (RDM; see Fig. 2A for party average RDMs). To compute intersubject similarity, we correlated a participant's RDM with every other participant's RDM, resulting in a group-level intersubject representational similarity matrix (IS-RSM) where each value in the matrix represents the similarity between political words for a particular subject dyad. To measure ideological affinity, we computed an ideological similarity score for each dyad on the basis of their self-reported political ideology score, ranging from *extremely liberal* to *extremely conservative* on a 100-point scale (*62*). We used this ideological closeness metric in a dyadic regression model (*17*), using a custom implementation of the linear mixed-effects regression approach described by Chen and colleagues [(*42*); see Methods]. As each observation in the regression represents a unique pair of participants, the model includes a random participant intercept for both participants in a dyad (*42*). In line with prior work (*23*, *24*), this dyadic regression revealed that increased similarity in the semantic representation of political words predicts ideological similarity [$\beta = 0.094 \pm 0.035$ (SE), $t(575.7) = 2.661$, $P = 0.006$; all reported P values are bootstrapped, see Methods; Fig. 2B].

To investigate whether these behavioral patterns are also reflected at the neural level, we test whether shared representation of political words in the brain predicts a shared ideological affinity. Leveraging intersubject RSAs [IS-RSAs; (*41*)] enables us to account for inherent statistical dependencies between dyads using linear mixed-effects modeling (*42*) in our a priori regions of interest (ROIs). Subject-level representational patterns were computed by calculating the cross-validated Mahalanobis distance (*63*) in activity patterns between words in each category (Fig. 1, purple arrow). Intersubject similarity in representational patterns was defined as the Pearson correlation between each pair of subjects' neural representational patterns for a given word category and ROI (Fig. 2C), which we then regressed onto ideological similarity (see Methods; Fig. 2D). This dyadic regression revealed that similar patterns of

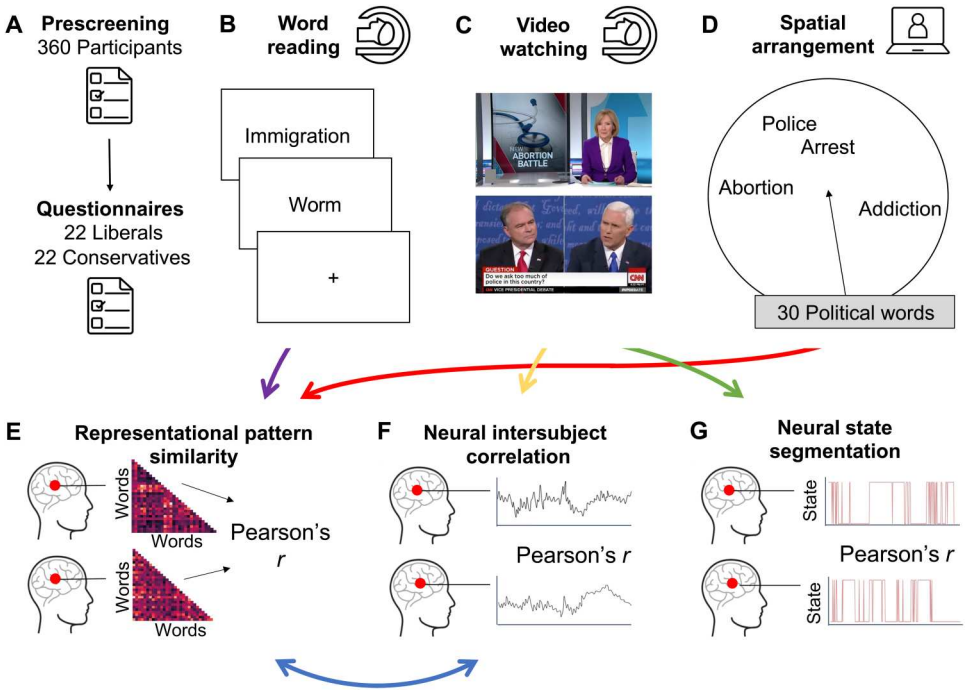

Fig. 1. Experimental structure. (**A**) Participants completed multiple questionnaires assessing political orientation and demographics before completing two tasks in the scanner—(**B**) a word reading task and (**C**) a video watching task. (**D**) A spatial arrangement task of the words presented in the word reading task was completed after the scanning session. Data collected during the word reading task (purple arrow) and the spatial arrangement task (red arrow) were used in (**E**) an RSA. For the video watching task, (**F**) neural intersubject correlation (ISC) (yellow arrow) and (**G**) neural state segmentation (green arrow) were computed. Representational pattern similarity was used to model neural ISC (blue arrow). Behavioral pattern similarity, neural pattern similarity, ISC, and neural state segmentation similarity were all used to model ideological similarity. Images in (C) are stills from the following video footage: PBS News Hour on the topic of abortion and CNN Vice-Presidential Debate coverage.

activity predict ideological similarity: patterns within the striatum for words in the categories "immigration" [$\beta = 0.071 \pm 0.035$ (SE), $t(784.5) = 2.046$, $P = 0.041$] and "American" [$\beta = 0.105 \pm 0.035$ (SE), $t(787.9) = 3.036$, $P = 0.003$], and patterns in the TPJ for words in the "American" category [$\beta = 0.130 \pm 0.035$ (SE), $t(803.9) = 3.745$, $P < 0.001$].

Given that both behavior on the spatial arrangement task and neural representations of words significantly predict ideology, we hypothesized that behavior on the spatial arrangement task should also predict neural representations. As the behavioral task forces participants to represent words in only two dimensions and within a circular space, we first transformed the neural representational patterns, which are likely higher dimensional, to a two-dimensional space by applying multidimensional scaling to the neural data (see Methods). To then test the relationship between these patterns at the behavioral and neural levels, we built a dyadic regression model where our IS-RSMs representing behavioral similarity in semantic distances between political words served as a predictor for the neural IS-RSMs representing similarity in activity patterns for each political category. We observed individuals exhibiting greater intersubject similarity for both political words and neural activity patterns in the striatum for words in the category "American" [$\beta = 0.085 \pm 0.034$ (SE), $t(859.0) = 2.498$, $P = 0.013$], an effect that remains significant when controlling for the unique effect of ideological similarity [$\beta = 0.088 \pm 0.034$ (SE), $t(858.0) = 2.579$, $P = 0.013$]. Together, these findings lend support to the hypothesis that shared semantic representations of political concepts on both the behavioral and the neural level predict ideological like-mindedness—even when these words are presented without any context.

Shared neural representations of political concepts predicts the processing of naturalistic political information

Although we found evidence that the manner in which political concepts are represented in the brain predicts whether two individuals share a political ideology, it remains unclear whether these abstract representations, elicited in a context-free and static task, also predict how dynamic, real-world political information is processed. That is, can individual differences in the neural representations of political words account for differences in the neural processing of naturalistic political content? To investigate this, we tested whether shared neural representations for relevant political words in the word reading task predict brain-to-brain synchrony in our a priori ROIs during the neutrally worded news clip on abortion and the Vice-Presidential Debate on policing and immigration (Fig. 1, blue arrow and Fig. 3A). Intersubject similarity in the activity patterns for words that correspond to the topics covered in the videos (e.g., *abortion*, *police*, and *immigration*) were used in a dyadic linear mixed-effects regression model to predict brain-to-brain synchrony during the videos (Fig. 1, yellow arrow; see Methods).

We found that individuals that exhibited more similar activity patterns for words in the category "immigration" during the word reading task exhibited greater intersubject correlation (ISC) in the amygdala during the part of the debate video that covered the topic of immigration [$\beta = 0.083 \pm 0.033$ (SE), $t(790.4) = 2.516$, $P = 0.029$; Fig. 3B], an effect that did not extend to the other topic covered in

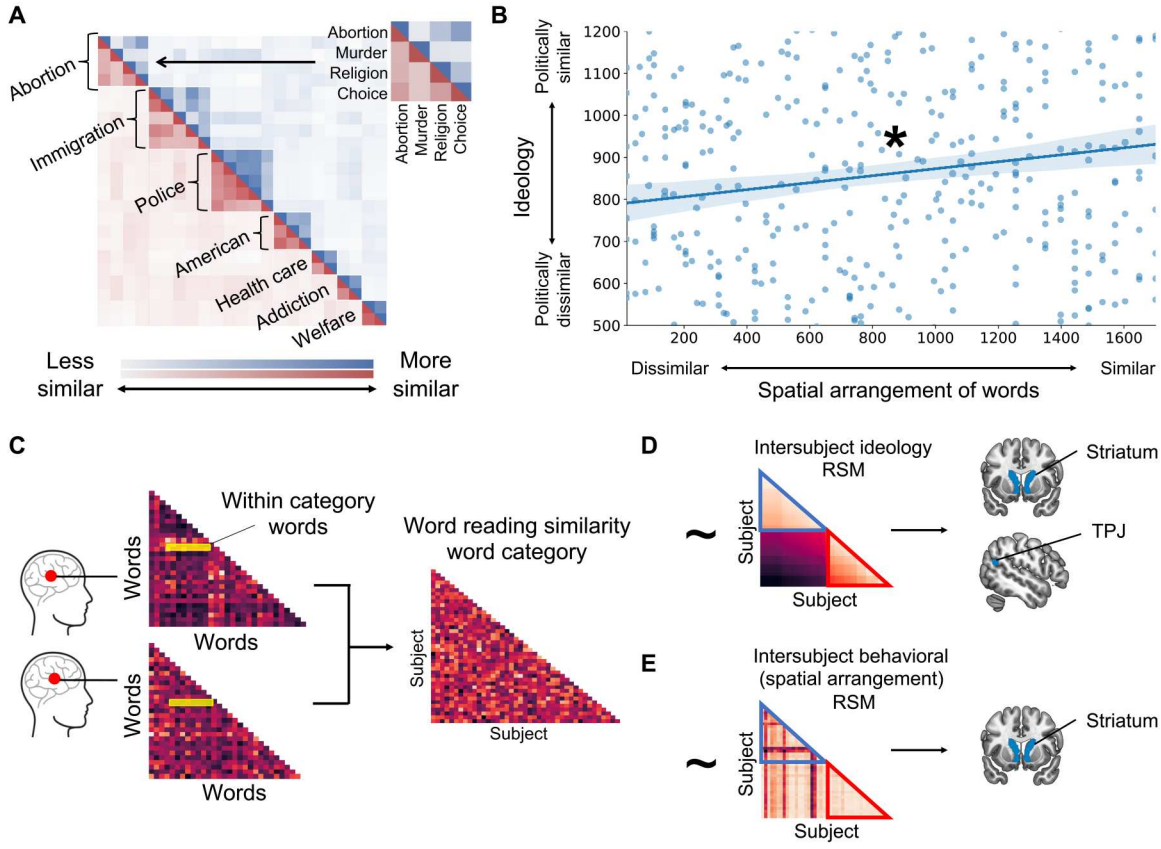

Fig. 2. Shared political ideology shapes intersubject similarity in the representational patterns of political words. (**A**) The average behavioral representational similarity matrices of the political words for the conservatives (red) and liberals (blue). For the neural word reading pattern analyses, only the within-category word pairs were analyzed. (**B**) Intersubject similarity in political ideology is predicted by intersubject similarity in the behavioral spatial arrangement of political words (ranked data points). *P< 0.01. (**C**) Intersubject similarity in the neural representation of political words within the same word category was computed and (**D**) used to model intersubject similarity in political ideology, which reveals a significant effect in the striatum and TPJ. (**E**) In addition, neural intersubject similarity was regressed onto intersubject similarity in the behavioral spatial arrangement of the political words, where we again found an effect in the striatum.

the debate (policing, $P = 0.123$). We observed a similar coupling between activity patterns for words related to "abortion" in the word reading task and neural synchrony during the news clip on the topic of abortion in the striatum [$\beta = 0.095 \pm 0.033$ (SE), $t(835.0) = 2.896$, $P = 0.004$; Fig. 3C] and at the level of a trend in the amygdala [$\beta = 0.055 \pm 0.034$ (SE), $t(857.3) = 1.626$, $P = 0.100$; see the Supplementary Materials for additional control analyses]. The effects for the "immigration" and "abortion" models were not significantly different from each other ($P = 0.819$) but were significantly stronger than the policing effect [immigration: $\beta = 0.114 \pm 0.048$ (SE), $t(1612.0) = 2.355$, $P = 0.020$; abortion: $\beta = -0.113 \pm 0.048$ (SE), $t(1668.4) = -2.338$, $P = 0.021$]. The fact that we only found effects for these topics aligns with the behavioral judgments obtained after subjects watched the videos, which revealed that the topic of immigration was the most polarizing, with abortion a close second (see the Supplementary Materials). These results are the first that we are aware of that provide evidence of a link between polarized semantic representations of political concepts in the brain and polarized interpretation of naturalistic political content.

Together, these findings show that behavioral and neural representations of political concepts are predictive of political ideology and that these representations predict intersubject synchrony during naturalistic political video watching. Given that prior literature shows how neural synchrony reflects ideological similarity (*12*, *17*, *18*), we capitalized on the two-task structure of our experimental paradigm to test whether neural synchrony predicts ideological similarity while controlling for the neural representations of political concepts. We thus used a dyadic regression to test the unique contributions of increasingly similar neural representations for political words in the word reading task and greater brain-to-brain synchrony during the naturalistic videos on whether two individuals exhibit a shared ideology. Leveraging the same logic in the analysis above, where related topics are tested in the same dyadic regression in our a priori ROIs (e.g., restricting analyses to words in a category that match the topically relevant portions in the videos), we observed that in the striatum, similar representations and synchronized BOLD time courses to the topic "immigration" predict increased ideological similarity [word reading task: $\beta = 0.070 \pm 0.034$ (SE), $t(783.6) = 2.030$, $P = 0.048$; ISC: $\beta = 0.106 \pm 0.035$ (SE), $t(740.2) = 2.990$, $P = 0.001$; see the Supplementary Materials for the full list of active regions]. This suggests that in the striatum, neural synchrony is partially shaped by neural representations of political concepts and that both

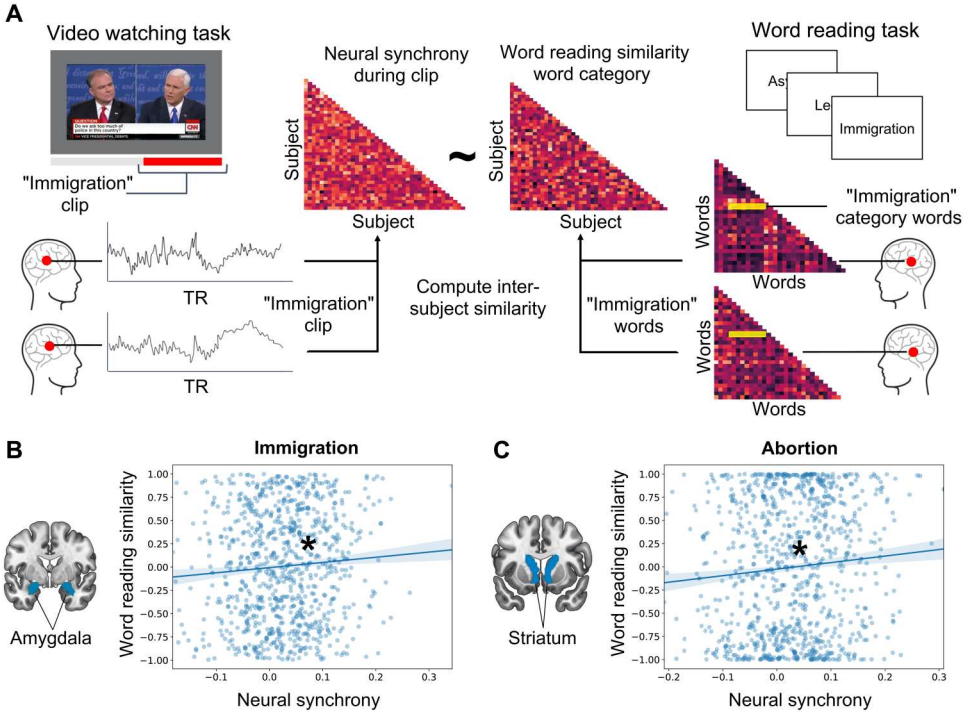

Fig. 3. Neural representational similarity of political words predicts neural intersubject similarity during naturalistic viewing of political content. (**A**) Neural intersubject similarity during a video clip on a politically charged topic (e.g., the immigration portion of the debate video) was computed and modeled using intersubject similarity in neural representational patterns of words from the word reading task that relate to the (immigration) topic. TR, repetition time. (**B**) Results reveal that neural synchrony (ISC) in the amygdala during the portion of the debate video that covered the topic of immigration was predicted by intersubject similarity in representational patterns of the word category "immigration" in the same region. (**C**) Neural synchrony in the striatum during the news clip on abortion was predicted by intersubject similarity in representational patterns of the word category "abortion" in this same region. Image in (A) is a still from CNN Vice-Presidential Debate coverage. *P< 0.05.

modalities—neural representations of concepts and neural synchrony of naturalistic content—significantly and independently predict ideological similarity.

The segmentation of naturalistic political content predicts shared ideology

While ISC is the most common and longstanding method used to probe shared interpretations, how the brain temporally segments perceptual inputs can also be leveraged to measure shared interpretations. This is because the temporal segmentation of incoming information reflects one's subjective parsing of an observed sequence of events (*36*–*38*). If like-minded partisans segment information in a similar way, then it would provide converging evidence that polarized beliefs stem from perceptual processing stages. To test this, we used a data-driven approach that identifies stable patterns of neural activity and hierarchically clusters them into distinct neural states [Fig. 1, green arrow; (*35*, *36*)]. An advantage of this approach is that we can fit the model to raw fMRI data in our ROIs without having to rely exclusively on human segmentation annotations. Hierarchical clustering was fit with two alternating states, given that two states provided the best fit to the data (see Methods). We then correlated each subject's temporal pattern of neural state switching during naturalistic video watching with those of all other subjects to assess whether the temporal synchronization of neural states correlates with ideological similarity (Figs. 1G and 4A). In the Vice-Presidential Debate segment that covered immigration, ideologically like-minded individuals exhibit greater temporal synchronization of neural states in the dmPFC, even when controlling for shared patterns of activity during the word reading task and interbrain correlations during the video [$\beta = 0.119 \pm 0.036$ (SE), $t(805.3) = 3.326$, $P = 0.002$; Fig. 4, B and C; see the Supplementary Materials for the full list of significant regions]. This relationship was not observed in the policing clip ($P = 0.658$) or neutrally worded video on abortion ($P = 0.294$).

To better understand whether these temporal states changes in the dmPFC reflect differences in affective experience between political parties, we linked these state change patterns to psychological measures provided by independent coders (collected before the scanning session). Coders were asked to rate each video fragment (at approximately 10-s intervals) on how much Democrats and Republicans would differ in their experiences along four dimensions: emotional agreement, agreement with the speaker, speaker's intentions, and agreement on semantic meaning. To test for partisan differences in affective and semantic experience, we computed temporal state pattern differences between political parties by applying the hierarchical clustering algorithm to the average neural BOLD signal across individuals within a given party and then transformed these to represent state changes, such that we could compute differences between state sequences at the party level (Fig. 5; see Methods). This difference in cross-party state change sequences was then linked to the ratings from the independent coders. For the portion of the debate that covered the topic of immigration, we found a significant correlation in temporal state changes along party lines for emotional disagreement (rho = 0.113, $P = 0.016$) and

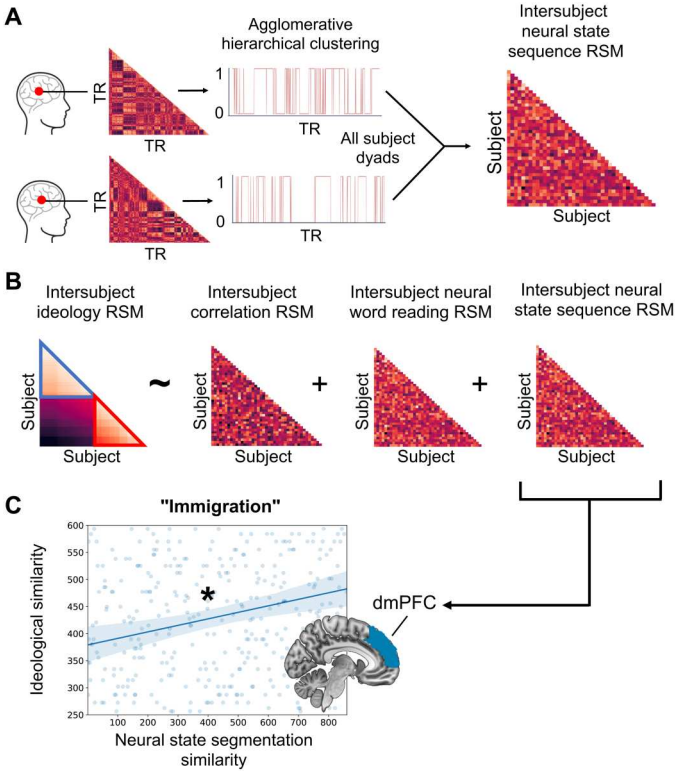

Fig. 4. Intersubject similarity in neural state segmentation during political video watching predicts shared political ideology. (**A**) For each subject, agglomerative hierarchical clustering was applied to the BOLD signal from ROIs, resulting in a sequence of two alternating neural states. These sequences of neural states were correlated across subjects, resulting in a subject-by-subject neural state sequence RSM. (**B**) Ideological similarity was modeled as a function of intersubject similarity in state sequences, ISC, and intersubject similarity in neural word reading patterns on the same topic. (**C**) Intersubject similarity in neural state patterns significantly predicts ideology in the dmPFC during the immigration topic, even while controlling for ISC and intersubject similarity in word reading for the same topic. *$P < 0.05$.

semantic disagreement (rho = 0.149, $P = 0.003$). That is, the differences in neural state change sequences between Democrats and Republicans appear to reflect partisan differences in emotionally and semantically distinct experiences. Together, this reveals that the temporal segmentation of naturalistic political narratives in the dmPFC likely relies on affective experiences shaped by individuals' political ideologies.

DISCUSSION

Ideological division and negative feelings between conservatives and liberals have risen sharply over the past few decades (*64*–*67*). Although we know that a lack of mutual understanding between parties is one factor driving political polarization (*27*, *67*), very little is known about how the brain comes to hold a polarized perspective (*1*). We propose a model of political polarization driven by shared semantic representations, synchronized neural responses, and aligned segmentation of neural states. Critically, we observe a link between how the brain represents static political concepts and how it experiences real-world political content, revealing that semantic knowledge shapes whether people come to share a polarized interpretation of naturalistic audio-visual stimuli consumed in context—a finding that supports that neural synchrony reflects, at least in part, a shared understanding (*68*). Moreover, partisans on opposite sides of the aisle experience discrete affective experiences that likely help segment real-world information into the same meaningful units. Simply put, despite receiving the same input, two individuals can arrive at politically opposing conclusions via a process shaped by how similarly they represent, interpret, and experience the same information. This builds on recent research demonstrating that shared political ideology is associated with increased neural synchronization during political video watching (*17*, *18*), suggesting that these effects are at least partly driven by having shared representations of political concepts and aligned temporal experiences of political narratives.

Specifically, we first observed that when encoding abstract political words (e.g., *immigration*), the more two individuals share an ideological perspective—be it liberal or conservative—the more they exhibit similar representational patterns in the striatum and TPJ. These increasingly similar neural patterns for the political words presented in the word reading task predicted more synchronized BOLD time courses in the striatum and amygdala when viewing real-world, dynamic political narratives. Second, a synchrony effect in the dmPFC was also observed during neural state segmentation: The segmentation of politically inflammatory information is most similar between like-minded ideologues, whether they fall on the left or right side of the aisle, an effect that appears to be driven by differences in emotional experiences and semantic understanding. Together, these findings reveal that political polarization arises from a combination of neural mechanisms that work in concert, including how people represent abstract political concepts, which, in turn, shapes how they process and segment ongoing information.

When two individuals' political ideologies align, the striatum—a region known to encode value (*45*, *48*)—exhibits similar patterns of neural activity when representing static political words. In contrast, individuals who hold different political beliefs exhibit dissimilar patterns of neural activity in the striatum, despite being presented with the same political word. This suggests that ideology shapes how political concepts are represented and valued, even when presented in a context devoid of inflammatory language or a polarizing agenda. Moreover, similarity between these neural representations in the word reading task predicted the degree to which two individuals exhibit a synchronized BOLD response in the striatum and amygdala when watching related naturalistic political content, hinting that how the brain affectively values certain hot-button political concepts shapes whether people come to hold a polarized perspective. The idea that political polarization is driven by how individuals emotionally experience and come to value political information is supported by the involvement of the striatum and amygdala, which appear to encode the representation of political words and synchronization of BOLD responses during naturalistic political content to predict a shared ideology (*46*, *69*–*72*). Future research can further manipulate whether the affective value of political content modulates activity in these regions or whether the amygdala and striatum play functional roles that extend beyond emotion and valuation.

The temporal segmentation of incoming naturalistic political information provides an additional avenue for how people come to

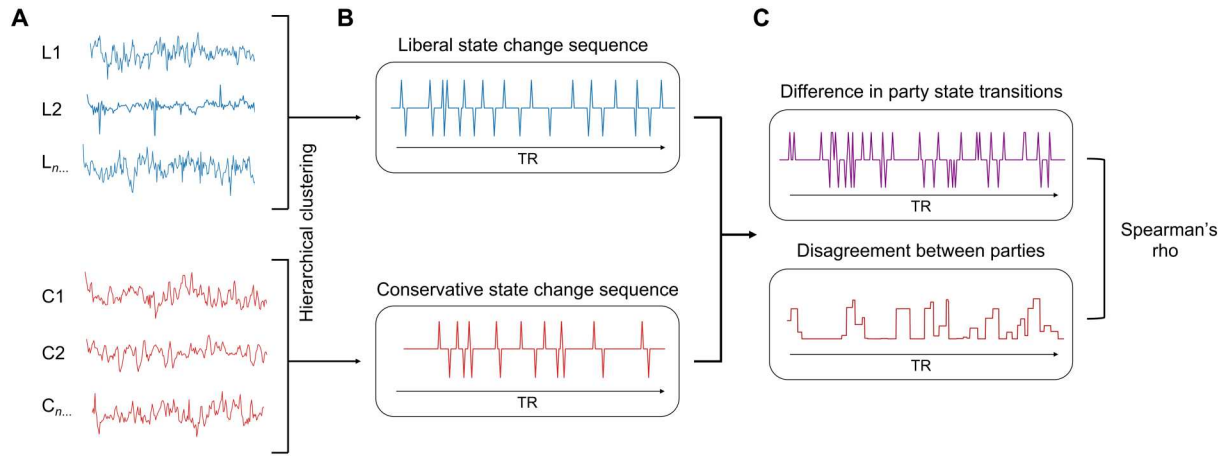

Fig. 5. Partisan differences in group-level state change patterns are associated with emotionally and semantically distinct experiences. (**A**) Party average neural BOLD signals were computed by averaging the neural signal across individuals within each political party. Hierarchical clustering was applied to these party average BOLD time courses, resulting in a liberal and conservative state sequence. (**B**) The state sequences were transformed to represent state changes by comparing the state at each time point (*t*) with the state at the time point before that (*t*−1). (**C**) Partisan differences in state transitions were computed by subtracting the absolute partisan state sequences from each other. The difference in party state transitions was Spearman correlated (see Methods) with disagreement ratings of the videos, provided by independent coders.

hold a polarized response. People help to make sense of a complex dynamic world by breaking up and structuring ongoing information into meaningful units. While controlling for neural representation and synchronization of BOLD time courses, we observed that the degree of similarity with which two individuals temporally segment ongoing political footage into smaller units in the dmPFC also predicts ideological similarity. The dmPFC, which is part of the mentalizing network (*56*, *57*) and plays an important role in understanding and taking the perspective of others, has recently been linked to political polarization (*18*). Thus, the dmPFC's involvement in segmenting incoming information in a politically polarized manner suggests that these synchronized neural processes may draw on the ability to perspective-take.

Together, these results hint at a neural model of polarized perception that is driven by a broad set of regions involved in affective valuation and mentalizing. Prior research has documented that regions involved in processing affect and theory of mind, mainly the amygdala, dmPFC, and TPJ, contribute to how social phenomena are valued (*73*). For example, we know that affective valuation depends on the coengagement of the amygdala and striatum (*74*–*78*), and greater functional coupling between theory of mind regions and the striatum is linked to increased prosocial decision-making (*79*). Our work extends this, revealing that both affect and perspective taking are involved in the subjective valuation of political information and, ultimately, a polarized view. Such a neural model of affective polarization dovetails with the growing body of research focusing on political polarization at the behavioral level, which documents that a polarized perception is strongly associated with altered emotional attitudes and behaviors toward political foes (*27*, *28*, *43*, *44*).

It is important to note that throughout our analyses, the topic of immigration elicited the strongest polarized response. That these effects did not extend to the other political topics is likely the result of the political climate at the time of data collection, which took place at the beginning of 2019, only a few months after D. Trump introduced the Build the Wall, Enforce the Law Act. At that time, immigration was widely covered in the media, and there were stark differences between the policies endorsed by Democrats and Republicans (*80*). The salience of this topic—in relation to the other political topics our study covered—was leveraged by other research conducted in the same time frame, which specifically focused on the topic of immigration due to its highly polarizing nature (*18*). Although the topics of policing and abortion are acutely relevant in today's political theater (e.g., the Black Lives Matter movement gained momentum in May 2020, and in 2021–2022, there were highly polarizing changes in abortion policies in America), these hot-button topics did not have as much media coverage when our data were collected. This may explain why most of our findings rest on the topic of immigration.

One persistent challenge when studying political polarization in the laboratory is that political content is highly complex and typically ignited in naturalistic conditions, such as watching TV or engaging in social media. We sidestepped these challenges by merging tightly controlled political stimuli with more dynamic and evolving political footage and measuring how static representations bias how humans process real, complex information on the fly. That political beliefs appear to be broadly affected by the way incoming political information is processed and valued across modalities (i.e., representation, segmentation, and BOLD time course) suggests that sharing a polarized political viewpoint is biased by multiple different levels of the cognitive processing stream. We propose a model of political polarization mainly driven by altered processing between opposing partisans in regions important for affective valuation and mentalizing. Given that political polarization poses great challenges to communication and cooperation between parties and hinders political decision-making by complicating compromises between ideological extremes (*81*–*84*), gaining a better understanding of how political polarization arises is of paramount importance.

METHODS

Participants

The data analyzed for this paper were collected as part of a larger study on political preferences. Via online advertisements, posters and flyers, and recruitment visits to political meetings, 360 potential participants were recruited and filled out a screening survey online. On the basis of a slider measure of ideology (*62*), 22 self-reported conservatives and 22 liberals were invited from this larger pool for an in-laboratory session. All participants were right-handed and MRI eligible. One participant was excluded from further analyses for indicating a different ideology on the screening survey versus the postscan political survey battery. This resulted in the inclusion of 21 conservatives [13 men and 8 women; age range 18 to 61, mean age = 36 ± 15 (SD) years] and 22 liberals [13 men and 9 women; age range 18 to 60, mean age = 28 ± 12 (SD) years], representing a range of ideological extremities. There were no significant differences in age, gender, education level (number of years completed), and annual income between the two groups (two-sample *t* tests, two-sided: all *P*s > 0.05; see the Supplementary Materials). Participants provided informed consent and received monetary compensation ($40) for participating in this study. The study procedures were approved by the Brown University Institutional Review Board.

Procedure

The total duration of the experiment was approximately 3 hours. Participants first updated their MRI screening information and were asked to read the instructions and answer comprehension questions. Participants then entered the MRI scanner for a scanning session of about 1.5 hours in which they completed two tasks: a word reading task and a video watching task. Between the two tasks, a 5-min anatomical scan was collected. To minimize head motion, soft padding was positioned around the head. Participants held the response button box in their right hand while skin conductance was measured using two electrodes placed on their left hand (not analyzed here). After the scanning session, participants again completed one of the tasks (video watching task, see below) outside of the MRI scanner.

Word reading task

In the scanner, participants first completed the word reading task. On each trial of the word reading task, participants read a word on the screen and indicated with a button press whether the word was political or nonpolitical. There were 60 unique words: 30 political and 30 nonpolitical (see the Supplementary Materials). The nonpolitical words were objects (15) and animals (15). The political words consisted of seven theme words, chosen for their polarizing nature and/or their occurrence in the political videos of the video watching task (see below), which included "abortion," "addiction," "American," "health care," "police," "immigration," and "welfare." The other 23 words were association words, chosen for their polarizing relationship to the theme words. To select the association words, we ran an experiment on Mechanical Turk (n = 101) where conservative and liberal individuals from the United States freely associated with the theme words by typing associated terms in a free-response box [a semantic fluency task, known to elicit partisan differences in associations (*24*); see the Supplementary Materials for details]. Each trial stimulus was presented for 2.5 s with a 2.5-s fixation cross in between. Twenty null trials were added (fixation cross) to ensure independent recoverability of the stimulus-evoked activity. Total block duration was around 6 min. Six blocks were presented, in which word presentation was randomized. During the task, participants were instructed to indicate whether a word was political or nonpolitical by pressing the buttons on the response button box.

Naturalistic video watching

The video watching task consisted of a fixed sequence of three videos, two of which were included in our analyses: a neutrally worded news item on abortion legislation (PBS News Hour, "State battles over abortion policy anticipate a post-Roe world," item of 7:23 min: www.pbs.org/newshour/show/state-battles-over-abortion-policy-anticipate-a-post-roe-world) and a politically charged clip of the 2016 Vice-Presidential debate between liberal Democrat T. Kaine and conservative Republican M. Pence [CNN, "Vice-Presidential Debate 2016," clip of 17:47 min (24:30 to 42:10): www.youtube.com/watch?v=ox8PTXwDYdc]. The videos were presented on a gray background screen, at 80% of the screen size. A fixation cross was shown before and between all videos.

Behavioral testing session

After the scanning session, participants completed a behavioral testing session, including a spatial arrangement task (*61*), a survey on video comprehension (not analyzed here) and judgment, and an extensive survey battery of political and cognitive questionnaires (not analyzed here). For the spatial arrangement task, subjects were instructed to order the same political words as were used in the word reading task in a two-dimensional space (circle) based on their semantic similarity. Words that were believed to be related to each other had to be placed close to each other, whereas words that were not associated had to be placed further apart. No other instructions about dimension or word placement were provided. This resulted in a grouping of the words based on a subject's belief of semantic similarity, which could then be used to assess which words subjects associated with each other. This method of measuring similarity has been extensively validated against other metrics of similarity (*61*, *85*).

Behavioral data analysis

Dyadic regression model

To link the different modalities that were used in this research, a dyadic regression model was used. This model is a custom implementation of the mixed-effects regression approach reported by Chen and colleagues (*42*) based on the packages lme4 1.1-23 and lmerTest 3.1-2 for R 3.5.2, but optimized to link behavioral measures, neural synchrony, RSA, and neural state segmentation. Because each observation in the mixed-effects regression corresponded to a unique pair of subjects, the model for each observation includes a random participant intercept for both participants involved in that participant pair (*42*). This enables us to account for inherent statistical dependencies between dyads. As this model uses similarity between participants rather than individual measures (e.g., neural or behavioral measures), it makes it possible to compare and combine results from different modalities into one regression model. Before running the linear mixed-effects regression, all regressors were *z*-scored. To increase the robustness of the dyadic regression results and to control for incidental findings (*86*), we applied bootstrapping to all dyadic regression analyses, using the boot.pval package (*87*) with a 95% confidence interval and 10.000 bootstrap replicates. All reported *P* values represent bootstrapped estimates.

Word reading task

Participants were instructed to categorize the 60 words as either political or nonpolitical by using the MRI response button box. On the basis of the behavioral ratings of the words as political or nonpolitical, words on which the average performance was less than 67% accuracy (at least four correct responses in the six runs) were excluded from further analyses. This resulted in the exclusion of seven political words—*hospital*, *death*, *sick*, *child*, *gambling*, *doctor*, and *family*—leaving 53 words included. For the included words, subjects were able to correctly group the presented words into political and nonpolitical words in 89.2 ± 8.5 percent of the trials. No party differences were found between the liberals and conservatives for any of the 53 included words (two-sample *t* tests, two-sided: all *P*s > 0.05; see the Supplementary Materials) or in average performance over all 53 words [$t(52) = 0.497$, $P = 0.620$].

Spatial arrangement task

For the spatial arrangement task, multidimensional scaling was used to transform the data from the word spatial arrangement task to values reflecting dissimilarities (*61*). On the basis of the placement of the political words, the Euclidean distance between all word pairs was computed as $\sqrt{(x_2 - x_1)^2 + (y_2 - y_1)^2}$, resulting in an RDM that represented the behavioral pairwise distances between all words. Intersubject similarity in behavioral representations was computed by correlating the lower triangles of the RDMs (Pearson correlation), resulting in a correlation value per subject dyad. To investigate whether behavioral similarity in political word representations predicted ideological similarity, ideological similarity was regressed onto intersubject similarity on the spatial arrangement task using the aforementioned dyadic regression model. Ideological similarity was computed as 100 − abs(ideology_1 − ideology_2), where 1 and 2 refer to the two participants in the current participant pair. Both intersubject similarity on the spatial arrangement task and ideological similarity were *z*-scored before running the model.

Judgments elicited by the videos

After watching the videos in the scanner, participants completed a questionnaire about how they felt about eight statements made in the videos (four in the abortion video and four in the debate video, two of which covered the topic of policing and two of which covered the topic of immigration). For each statement, participants were asked to indicate how much they agreed or disagreed with the statement on a seven-point Likert scale. First, two-sample *t* tests were conducted for each statement to test for partisan disagreement. Second, we tested whether there was an interaction effect between topic and political party for these ratings. The scores were first transformed so that higher scores represented a positive attitude toward the topic and then averaged for each topic. We then divided the eight statements into a two-by-three analysis of variance (ANOVA) to test for a significant interaction effect of political ideology by topic. To further understand the relationships between these two variables, additional two-by-two ANOVAs were conducted for the different combinations of the topics.

fMRI acquisition

MR images were acquired on a Siemens Prisma Fit 3-Tesla research-dedicated scanner (Siemens Healthineers, Erlangen, Germany) at the Carney Institute for Brain Science at Brown University. A 64-channel head coil was used to collect the fMRI data. T2*-weighted functional scans were acquired using Simultaneous Multi-Slicing, resulting in a factor of 3 scan time reduction. This increases the number of time points and thus statistical power for brain-to-brain temporal synchrony analysis. Echo planar images covering the entire brain except part of the cerebellum were acquired using contrast settings optimized from cortical gray matter [Repetition Time (TR)/Echo Time (TE)] 1500/30 ms, voxel size 3-mm isotropic, 64 × 64 voxels, flip angle 86°, 60 slices, and distance factor 0%). The field of view was tilted upward by 25° at the front of the brain to minimize tissue gradient–related signal dropout in the orbitofrontal cortex. To acquire a three-dimensional T1 anatomical scan, the magnetization-prepared rapid acquisition gradient-echo imaging sequence (*88*) was used [TR/TE/Inversion Time (TI) 1900/3.02/900 ms, voxel size 1-mm isotropic, 256 × 256 voxels, parallel imaging (GRAPPA 2), flip angle 9°, 160 slices, and distance factor 50%].

fMRI preprocessing

Results included in this manuscript come from preprocessing performed using fMRIPrep 1.5.1rc2 [RRID:SCR_016216; (*89*, *90*)], which is based on Nipype 1.3.0-rc1 [RRID:SCR_002502; (*91*, *92*)]. The complete preprocessing pipeline can be found in the Supplementary Materials. The anatomical T1-weighted (T1w) images were corrected for intensity nonuniformity, distributed, and used as T1w reference image. After skull stripping, brain tissue segmentation was performed, and the T1w images were transformed to standard space (MNI152Nlin2009cAsym). For each of the eight functional BOLD runs per subject (across all tasks and sessions), a reference volume and its skull-stripped version were generated using a custom methodology of fMRIPrep. The functional images were coregistered to the T1w images and normalized. Slice time correction and motion correction were applied. Physiological noise regressors were extracted using CompCor (*93*), which estimates both temporal and anatomical principal components. The six BOLD runs collected during the word reading task were not susceptibility distortion corrected in the absence of inhomogeneity fieldmaps. After preprocessing, smoothing was applied to these six runs, using a 6-mm full width at half maximum Gaussian smoothing kernel and implicit brain masking in SPM12.

fMRI data cleaning

For the word reading task, runs in which there were excessive motion artifacts or in which subjects did not press the response button for multiple word representations, which was interpreted as a lack of attention, were excluded. This resulted in a total exclusion of nine runs from seven subjects (on average 1.4 run per subject) and the exclusion of one subject all together.

One participant′s data were excluded from analysis for the debate video because of excessive head motion. All other functional fMRI data were further preprocessed using nltools 0.3.14 (*94*) to remove signal components related to motion and other sources of noise. General linear models of each voxel′s signal time series were constructed with the following regressors: average cerebrospinal fluid signal; average white matter signal; the six realignment parameters, their derivatives, their squares, and their squared derivatives (*95*); zero-, first-, and second-order polynomials for removal of intercepts and linear/quadratic trends; and a regressor for each motion spike, which has value 1 at the TR where the spike was detected [Framewise Displacement (FD) > 1 mm] and zeros elsewhere.

The residual time series of each voxel were then used for statistical analysis.

Statistical fMRI analysis

Word reading task

An ROI-based IS-RSA (*41*) was conducted for the word reading task. Five preregistered ROIs (https://osf.io/zsjdc/) were selected on the basis of their functional association with mentalizing (TPJ and dmPFC) and affective valuation [striatum, amygdala; (*12*, *45*–*49*, *56*–*59*)] and semantic processing [middle temporal gyrus; (*68*, *96*–*98*)]. ROIs were defined either as 6-mm spheres around a center voxel coordinate taken from prior research or by using the Automated Anatomic Labelling atlas (*99*) in the WFU Pickatlas toolbox for SPM12 [(*100*, *101*); see the Supplementary Materials for more details on the ROI definitions].

To extract word-related brain activation, a general linear model was constructed for each participant in which each word from each run of the word reading task was modeled as a separate regressor. This resulted in a beta map per run per word representing the spatiotemporal neural patterns elicited by that specific word. For each ROI, the beta values in the ROI voxels were extracted. To estimate representational dissimilarity between each pair of words from these regional word activations, we computed the cross-validated Mahalanobis distance (*63*) between all word pairs using the RSA Toolbox [http://github.com/rsagroup/rsatoolbox; (*102*)] in Matlab R2017b (The MathWorks Inc., www.mathworks.com). This method capitalizes on the separate observations from each run to establish a cleaner (cross-validated) approximation of the true neural representation of each word (*63*). This resulted in a neural word-by-word RDM for each ROI. From these neural RDMs, as with the behavioral data, the values representing within word-category word pairs were selected for each word category. Because of the exclusion of seven political words based on their inconsistent behavioral ratings at being political—*hospital*, *death*, *sick*, *child*, *gambling*, *doctor*, and *family*—we ended up with four categories consisting of more than two words: "abortion," "immigration," "police," and "American." These four category RDMs were used for further analyses.

To test what drove similarity in political ideology, we again applied the aforementioned dyadic linear mixed-effects regression model (*17*, *42*). In this analysis, we computed the neural intersubject similarity of the word representations (Pearson correlation) between each pair of subjects for each word category. We analyzed these observations in two distinct ways, each testing a different hypothesis. First, to test the relationship between ideological similarity and similarity in the neural representation of political words, we modeled ideological similarity as a function of pairwise neural similarity values and random participant intercepts, for each word category separately. Second, to investigate the association between behavioral intersubject similarity (in how participants placed the words on the spatial arrangement task) and word representational similarity, we regressed intersubject similarity in neural word representations for each word category onto intersubject similarity on the behavioral spatial arrangement task. For each ROI, the subject-level neural word-by-word RDMs were fitted and transformed to two-dimensional space using multidimensional scaling. Intersubject similarity in neural representational patterns was computed as described above, which was then regressed onto intersubject similarity in behavioral word representations. In addition to the bootstrapping, we also applied Bonferroni correction to all regression models to correct for the inclusion of five ROIs. These statistics can be found in the Supplementary Materials.

Video watching task

For the video watching task, we again used an ROI approach. To investigate the link between the word reading task and the video watching task, a dyadic regression model was used to model neural ISC during the videos using intersubject similarity in representational word patterns for words on a topic discussed in the video. For the debate video, the video was split up into two clips, with the first clip covering the topic of policing (start of the video until 09:56) and the second clip covering a discussion on immigration policies (09:57 to 17:47). For the news item video, the whole video was used as clip covering abortion policies. Similar to the approach described before, ISC in the preregistered ROIs was computed by extracting the average BOLD signal time course for each clip and computing the Pearson correlation between all subject dyads. For the word representational patterns, within-category representational similarity in each ROI was computed for the word categories discussed in the three different clips (i.e., "police," "immigration," and "abortion") by selecting the values of each subject's ROI neural RDM representing words from that word category and computing the Pearson correlation between these values for all subject pairs. These measures of representational similarity were *z*-scored and used in the before described dyadic linear regression model to try to model neural ISC in the same region during the corresponding video clip. To test whether the effects of the regression models for the included word categories were statistically different from each other, we ran additional dyadic regression analyses in which we tested for an interaction effect between the word category (dummy coded) and the predictive effect of word reading similarity on intersubject similarity during the video watching task. To test whether these two different measures of shared processing, measured during both static and naturalistic contexts, could predict ideological similarity, we modeled ideological similarity as a function of neural ISC and word representational patterns in the same ROI and covering the same topic, similar to the analysis described before.

The data-driven neural state segmentation approach to investigate possible partisan differences in neural states was based on work by Baldassano and colleagues (*35*) and Chang and colleagues (*36*). Although initial work describes states as sequential events based on specific narrative events (*35*), we define neural states as capturing distinct psychological processes, aligned with the definitions used by Chang and colleagues (*36*). For each of the preregistered ROIs, only voxels for which at least 80% of the subjects had data were included. For these included voxels, the BOLD patterns were extracted. Agglomerative hierarchical clustering was performed using the Scikit-learn toolbox in Python to segment the voxel time series into a temporal pattern of recurring neural states. To identify the number of states that best fit the data, the hierarchical clustering was fitted for each subject individually with all possible number of clusters, ranging from two to the total number of TRs in the video (debate video, 720 TRs; news item, 307 TRs). For each number of clusters, the Silhouette Score was computed as a measure of clustering accuracy (*103*). These silhouette scores were used to find the best-fitting number of clusters for each participant. Across all preregistered ROIs, two clusters best explained the data, which was computed by calculating the mode of the best-fitting

number of states across participants. No partisan differences in the best-fitting number of clusters were found (two-sample *t* tests, two-sided: all *P*s > 0.05; see the Supplementary Materials). Each subjects' voxel time series was used to compute a subject specific TR x TR correlation distance matrix, which incorporated spatial *z* scoring of the neural patterns. Agglomerative hierarchical clustering was then applied to each subjects' distance matrix with two clusters, resulting in a sequence of 0's and 1's representing a cluster or neural state for each time point (TR) in the video. This assumes that the participants cycled between two internal states, which likely glosses over subtleties of human experience but is nevertheless useful for lifting out higher-level shifts in emotional and/or cognitive experience [e.g., liking and disliking; (*36*)].

The aforementioned dyadic mixed-effects regression model was again used to investigate whether intersubject similarity in neural state sequences could predict ideological similarity. This was done separately for the immigration and policing part of the video. As a measure of intersubject similarity in neural state sequence, the absolute Pearson correlation between all subject dyads was computed. Because the hierarchical clustering was applied to each subject's data separately, the labeling of the states (0 or 1) was not aligned across subjects. By computing the absolute correlation between the state sequences, we created a measure of alignment of states, independent of their labeling. Unsynchronized state sequences were thus close to zero, whereas synchronized state sequences were represented by higher values. Theses state sequence similarities were then modeled as a function of ideological similarity while also controlling for neural word representational pattern similarity and ISCs of the BOLD signal.

To investigate what these temporal state change patterns might reflect on a psychological level, we linked these patterns to measures of the videos collected before the scanning sessions. Five independent coders watched the political videos and rated every 10-s video fragment on a scale of 0 to 10 on how much Democrats and Republicans would differ in their experience along four dimensions: emotional agreement, agreement with the speaker, speaker's intentions, and agreement on semantic meaning. These ratings were then *z*-scored, averaged across raters, and convolved with a function representing the hemodynamic response function (*104*) to match the temporal dynamics of the fMRI signal. To test for potential partisan differences, we computed temporal state pattern differences between political parties by first applying the hierarchical clustering algorithm to the average neural BOLD signal across individuals within a given party. To compare the state sequences between the two parties, sequences were then transformed to represent state changes, such that each state at time point *t* was compared with the state at the time point before that (*t*−1). We then computed the difference between the absolute partisan state change sequences, as the directionality of the state change was not of interest. This difference in cross-party state change sequences was then Spearman correlated with the ratings from the independent coders while applying phase randomization and 10,000 permutations using the nltools package (*94*).

Supplementary Materials

This PDF file includes:

Supplementary Text Tables S1 to S4
Fig. S1
References

View/request a protocol for this paper from *Bio-protocol*.

REFERENCES AND NOTES

1. J. M. van Baar, O. FeldmanHall, The polarized mind in context: Interdisciplinary approaches to the psychology of political polarization. *Am. Psychol.* **77**, 394–408 (2022).
2. N. J. Stroud, Polarization and partisan selective exposure. *J. Commun.* **60**, 556–576 (2010).
3. E. Pariser, *The Filter Bubble: How The New Personalized Web is Changing What We Read and How We Think* (Penguin Books, 2011).
4. A. J. Stewart, M. Mosleh, M. Diakonova, A. A. Arechar, D. G. Rand, J. B. Plotkin, Information gerrymandering and undemocratic decisions. *Nature* **573**, 117–121 (2019).
5. E. Bakshy, S. Messing, L. A. Adamic, Exposure to ideologically diverse news and opinion on Facebook. *Science* **348**, 1130–1132 (2015).
6. J. A. Frimer, L. J. Skitka, M. Motyl, Liberals and conservatives are similarly motivated to avoid exposure to one another's opinions. *J. Exp. Soc. Psychol.* **72**, 1–12 (2017).
7. R. K. Garrett, Echo chambers online?: Politically motivated selective exposure among Internet news users. *J Comput-Mediat.* **14**, 265–285 (2009).
8. C. G. Lord, L. Ross, M. R. Lepper, Biased assimilation and attitude polarization: The effects of prior theories on subsequently considered evidence. *J. Pers. Soc. Psychol.* **37**, 2098–2109 (1979).
9. M. L. Stanley, P. Henne, B. W. Yang, F. De Brigard, Resistance to position change, motivated reasoning, and polarization. *Polit. Behav.* **42**, 891–913 (2020).
10. S. Flaxman, S. Goel, J. M. Rao, Filter bubbles, echo chambers, and online news consumption. *Public Opin. Q.* **80**, 298–320 (2016).
11. C. A. Bail, L. P. Argyle, T. W. Brown, J. P. Bumpus, H. Chen, M. B. F. Hunzaker, J. Lee, M. Mann, F. Merhout, A. Volfovsky, Exposure to opposing views on social media can increase political polarization. *Proc. Natl. Acad. Sci. U.S.A.* **115**, 9216–9221 (2018).
12. Y. Yeshurun, S. Swanson, E. Simony, J. Chen, C. Lazaridi, C. J. Honey, U. Hasson, Same story, different story: The neural representation of interpretive frameworks. *Psychol. Sci.* **28**, 307–319 (2017).
13. R. P. Vallone, L. Ross, M. R. Lepper, The hostile media phenomenon: Biased perception and perceptions of media bias in coverage of the Beirut massacre. *J. Pers. Soc. Psychol.* **49**, 577–585 (1985).
14. A. H. Hastorf, H. Cantril, They saw a game; A case study. *J. Abnorm. Soc. Psychol.* **49**, 129–134 (1954).
15. B. J. Gaines, J. H. Kuklinski, P. J. Quirk, B. Peyton, J. Verkuilen, Same facts, different interpretations: Partisan motivation and opinion on Iraq. *J. Theor. Polit.* **69**, 957–974 (2007).
16. E. M. Caruso, N. L. Mead, E. Balcetis, Political partisanship influences perception of biracial candidates' skin tone. *Proc. Natl. Acad. Sci. U.S.A.* **106**, 20168–20173 (2009).
17. J. M. Van Baar, D. J. Halpern, O. FeldmanHall, Intolerance of uncertainty modulates brain-to-brain synchrony during politically polarized perception. *Proc. Natl. Acad. Sci. U.S.A.* **118**, e2022491118 (2021).
18. Y. C. Leong, J. Chen, R. Willer, J. Zaki, Conservative and liberal attitudes drive polarized neural responses to political content. *Proc. Natl. Acad. Sci. U.S.A.* **117**, 27731–27739 (2020).
19. T. Wheatley, O. Kang, C. Parkinson, C. E. Looser, From mind perception to mental connection: Synchrony as a mechanism for social understanding. *Soc. Personal. Psychol. Compass.* **6**, 589–606 (2012).
20. A. Baimel, S. A. J. Birch, A. Norenzayan, Coordinating bodies and minds: Behavioral synchrony fosters mentalizing. *J. Exp. Soc. Psychol.* **74**, 281–290 (2018).
21. M. Nguyen, T. Vanderwal, U. Hasson, Shared understanding of narratives is correlated with shared neural responses. *Neuroimage* **184**, 161–170 (2019).
22. T. Wheatley, A. Boncz, I. Toni, A. Stolk, Beyond the isolated brain: The promise and challenge of interacting minds. *Neuron* **103**, 186–188 (2019).
23. P. Li, B. Schloss, D. J. Follmer, Speaking two "Languages" in America: A semantic space analysis of how presidential candidates and their supporters represent abstract political concepts differently. *Behav. Res. Methods* **49**, 1668–1685 (2017).
24. D. J. Halpern, P. L. Rodríguez, Partisan representations: Partisan differences in semantic representations and their role in attitude judgments. *CogSci.* **2018**, 445–450 (2018).
25. M. Ponari, C. F. Norbury, G. Vigliocco, Acquisition of abstract concepts is influenced by emotional valence. *Dev. Sci.* **21**, e12549 (2018).
26. S.-T. Kousta, G. Vigliocco, D. P. Vinson, M. Andrews, E. Del Campo, The representation of abstract words: Why emotion matters. *J. Exp. Psychol. Gen.* **140**, 14–34 (2011).
27. S. Iyengar, Y. Lelkes, M. Levendusky, N. Malhotra, S. J. Westwood, The origins and consequences of affective polarization in the United States. *Annu. Rev. Polit. Sci.* **22**, 129–146 (2019).

28. J. N. Druckman, S. Klar, Y. Krupnikov, M. Levendusky, J. B. Ryan, Affective polarization, local contexts and public opinion in America. *Nat. Hum. Behav.* **5**, 28–38 (2021).
29. G. Vigliocco, L. Meteyard, M. Andrews, S. Kousta, Toward a theory of semantic representation. *Lang Cogn.* **1**, 219–247 (2009).
30. M. Gentzkow, J. M. Shapiro, M. Taddy, Measuring group differences in high-dimensional choices: Method and application to congressional speech. *Econometrica* **87**, 1307–1340 (2019).
31. J. Diedrichsen, N. Kriegeskorte, Representational models: A common framework for understanding encoding, pattern-component, and representational-similarity analysis. *PLOS Comput. Biol.* **13**, e1005508 (2017).
32. N. Kriegeskorte, J. Diedrichsen, Peeling the onion of brain representations. *Annu. Rev. Neurosci.* **42**, 407–432 (2019).
33. I. Charest, R. A. Kievit, T. W. Schmitz, D. Deca, N. Kriegeskorte, Unique semantic space in the brain of each beholder predicts perceived similarity. *Proc. Natl. Acad. Sci. U.S.A.* **111**, 14565–14570 (2014).
34. J. M. Zacks, N. K. Speer, K. M. Swallow, T. S. Braver, J. R. Reynolds, Event perception: A mind-brain perspective. *Psychol. Bull.* **133**, 273–293 (2007).
35. C. Baldassano, J. Chen, A. Zadbood, J. W. Pillow, U. Hasson, K. A. Norman, Discovering event structure in continuous narrative perception and memory. *Neuron* **95**, 709–721.e5 (2017).
36. L. J. Chang, E. Jolly, J. H. Cheong, K. M. Rapuano, N. Greenstein, P.-H. A. Chen, J. R. Manning, Endogenous variation in ventromedial prefrontal cortex state dynamics during naturalistic viewing reflects affective experience. *Sci. Adv.* **7**, eabf7129 (2021).
37. J. N. van der Meer, M. Breakspear, L. J. Chang, S. Sonkusare, L. Cocchi, Movie viewing elicits rich and reliable brain state dynamics. *Nat. Commun.* **11**, 5004 (2020).
38. H. R. Bailey, C. A. Kurby, J. Q. Sargent, J. M. Zacks, Attentional focus affects how events are segmented and updated in narrative reading. *Mem. Cognit.* **45**, 940–955 (2017).
39. C. M. Massad, M. Hubbard, D. Newtson, Selective perception of events. *J. Exp. Soc. Psychol.* **15**, 513–532 (1979).
40. N. Kriegeskorte, M. Mur, P. Bandettini, Representational similarity analysis - Connecting the branches of systems neuroscience. *Front. Syst. Neurosci.* **2**, 4 (2008).
41. J. M. Van Baar, L. J. Chang, A. G. Sanfey, The computational and neural substrates of moral strategies in social decision-making. *Nat. Commun.* **10**, 1483 (2019).
42. G. Chen, P. A. Taylor, Y.-W. Shin, R. C. Reynolds, R. W. Cox, Untangling the relatedness among correlations, Part II: Inter-subject correlation group analysis through linear mixed-effects modeling. *Neuroimage* **147**, 825–840 (2017).
43. S. Iyengar, G. Sood, Y. Lelkes, Affect, not ideology: A social identity perspective on polarization. *Public Opin. Q.* **76**, 405–431 (2012).
44. E. J. Finkel, C. A. Bail, M. Cikara, P. H. Ditto, S. Iyengar, S. Klar, L. Mason, M. C. McGrath, B. Nyhan, D. G. Rand, L. J. Skitka, J. A. Tucker, J. J. Van Bavel, C. S. Wang, J. N. Druckman, Political sectarianism in America. *Science* **370**, 533–536 (2020).
45. R. N. Cardinal, J. A. Parkinson, J. Hall, B. J. Everitt, Emotion and motivation: The role of the amygdala, ventral striatum, and prefrontal cortex. *Neurosci. Biobehav. Rev.* **26**, 321–352 (2002).
46. M. Davis, P. J. Whalen, The amygdala: Vigilance and emotion. *Mol. Psychiatry* **6**, 13–34 (2001).
47. M. Gallagher, A. A. Chiba, The amygdala and emotion. *Curr. Opin. Neurobiol.* **6**, 221–227 (1996).
48. S. N. Haber, Neuroanatomy of Reward: A view from the ventral striatum, in *Neurobiology of Sensation and Reward*, J. A. Gottfried, Ed. (CRC Press/Taylor & Francis, 2011).
49. M. R. Delgado, Reward-related responses in the human striatum. *Ann. N. Y. Acad. Sci.* **1104**, 70–88 (2007).
50. J. T. Kaplan, S. I. Gimbel, S. Harris, Neural correlates of maintaining one's political beliefs in the face of counterevidence. *Sci. Rep.* **6**, 39589 (2016).
51. N. O. Rule, J. B. Freeman, J. M. Moran, J. D. E. Gabrieli, R. B. Adams, N. Ambady, Voting behavior is reflected in amygdala response across cultures. *Soc. Cogn. Affect. Neurosci.* **5**, 349–355 (2010).
52. S. Clifford, How emotional frames moralize and polarize political attitudes. *Polit. Psychol.* **40**, 75–91 (2019).
53. J. Graham, J. Haidt, B. A. Nosek, Liberals and conservatives rely on different sets of moral foundations. *J. Pers. Soc. Psychol.* **96**, 1029–1046 (2009).
54. S. P. Koleva, J. Graham, R. Iyer, P. H. Ditto, J. Haidt, Tracing the threads: How five moral concerns (especially Purity) help explain culture war attitudes. *J. Res. Pers.* **46**, 184–194 (2012).
55. L. J. Skitka, C. W. Bauman, Moral conviction and political engagement. *Polit. Psychol.* **29**, 29–54 (2008).
56. D. M. Amodio, C. D. Frith, Meeting of minds: The medial frontal cortex and social cognition. *Nat. Rev. Neurosci.* **7**, 268–277 (2006).
57. C. D. Frith, U. Frith, The neural basis of mentalizing. *Neuron* **50**, 531–534 (2006).
58. R. Saxe, N. Kanwisher, People thinking about thinking people. The role of the temporo-parietal junction in "theory of mind". *Neuroimage* **19**, 1835–1842 (2003).
59. F. Van Overwalle, K. Baetens, Understanding others' actions and goals by mirror and mentalizing systems: A meta-analysis. *Neuroimage* **48**, 564–584 (2009).
60. S. A. Nastase, A. Goldstein, U. Hasson, Keep it real: Rethinking the primacy of experimental control in cognitive neuroscience. *Neuroimage* **222**, 117254 (2020).
61. N. Kriegeskorte, M. Mur, Inverse MDS: Inferring dissimilarity structure from multiple item arrangements. *Front. Psychol.* **3**, 245 (2012).
62. M. D. Dodd, A. Balzer, C. M. Jacobs, M. W. Gruszczynski, K. B. Smith, J. R. Hibbing, The political left rolls with the good and the political right confronts the bad: Connecting physiology and cognition to preferences. *Philos. Trans. R. Soc. Lond. B Biol. Sci.* **367**, 640–649 (2012).
63. A. Walther, H. Nili, N. Ejaz, A. Alink, N. Kriegeskorte, J. Diedrichsen, Reliability of dissimilarity measures for multi-voxel pattern analysis. *Neuroimage* **137**, 188–200 (2016).
64. A. I. Abramowitz, K. L. Saunders, Is polarization a myth? *J. Theor. Polit.* **70**, 542–555 (2008).
65. M. J. Hetherington, Resurgent mass partisanship: The role of elite polarization. *Am. Polit. Sci. Rev.* **95**, 619–631 (2001).
66. J. Westfall, L. Van Boven, J. R. Chambers, C. M. Judd, Perceiving political polarization in the United States: Party identity strength and attitude extremity exacerbate the perceived partisan divide. *Perspect. Psychol. Sci.* **10**, 145–158 (2015).
67. S. Iyengar, M. Krupenkin, The strengthening of partisan affect. *Polit. Psychol.* **39**, 201–218 (2018).
68. S. Dikker, L. J. Silbert, U. Hasson, J. D. Zevin, On the same wavelength: Predictable language enhances speaker-listener brain-to-brain synchrony in posterior superior temporal gyrus. *J. Neurosci.* **34**, 6267–6272 (2014).
69. E. A. Phelps, J. E. LeDoux, Contributions of the amygdala to emotion processing: From animal models to human behavior. *Neuron* **48**, 175–187 (2005).
70. J. E. LeDoux, *The Emotional Brain: The Mysterious Underpinnings of Emotional Life* (Simon & Schuster, 1996).
71. K. Sergerie, C. Chochol, J. L. Armony, The role of the amygdala in emotional processing: A quantitative meta-analysis of functional neuroimaging studies. *Neurosci. Biobehav. Rev.* **32**, 811–830 (2008).
72. J. E. LeDoux, Emotion circuits in the brain. *Annu. Rev. Neurosci.* **23**, 155–184 (2000).
73. C. C. Ruff, E. Fehr, The neurobiology of rewards and values in social decision making. *Nat. Rev. Neurosci.* **15**, 549–562 (2014).
74. G. G. Berntson, G. J. Norman, A. Bechara, J. Bruss, D. Tranel, J. T. Cacioppo, The insula and evaluative processes. *Psychol. Sci.* **22**, 80–86 (2011).
75. R. Adolphs, What does the amygdala contribute to social cognition? *Ann. N. Y. Acad. Sci.* **1191**, 42–61 (2010).
76. R. Hurlemann, A. Patin, O. A. Onur, M. X. Cohen, T. Baumgartner, S. Metzler, I. Dziobek, J. Gallinat, M. Wagner, W. Maier, K. M. Kendrick, Oxytocin enhances amygdala-dependent, socially reinforced learning and emotional empathy in humans. *J. Neurosci.* **30**, 4999–5007 (2010).
77. C. Civai, A. Sanfey, Mentalizing in value-based social decision-making: Shaping expectations and social norms, in *The Neural Basis of Mentalizing,* M. Gilead and K. Ochsner, Eds.(Springer International Publishing, 2021), pp. 503–516.
78. S. Evans, S. M. Fleming, R. J. Dolan, B. B. Averbeck, Effects of emotional preferences on value-based decision-making are mediated by mentalizing and not reward networks. *J. Cogn. Neurosci.* **23**, 2197–2210 (2011).
79. E. H. Telzer, C. L. Masten, E. T. Berkman, M. D. Lieberman, A. J. Fuligni, Neural regions associated with self control and mentalizing are recruited during prosocial behaviors towards the family. *Neuroimage* **58**, 242–249 (2011).
80. A. Daniller, Americans' immigration policy priorities: Divisions between – and within – the two parties (2019); www.pewresearch.org/fact-tank/2019/11/12/americans-immigration-policy-priorities-divisions-between-and-within-the-two-parties/.
81. D. Baldassarri, A. Gelman, Partisans without constraint: Political polarization and trends in American public opinion. *Am. J. Sociol.* **114**, 408–446 (2008).
82. A. Gutmann, D. Thompson, The mindsets of political compromise. *Perspect. Politics.* **8**, 1125–1143 (2010).
83. P. Mcavoy, D. Hess, Classroom deliberation in an era of political polarization. *Curric. Inq.* **43**, 14–47 (2013).
84. R. Y. Shapiro, Y. Bloch-Elkon, Do the facts speak for themselves? Partisan disagreement as a challenge to democratic competence. *Crit. Rev.* **20**, 115–139 (2008).
85. R. Richie, B. White, S. Bhatia, M. C. Hout, The spatial arrangement method of measuring similarity can capture high-dimensional semantic structures. *Behav. Res. Methods* **52**, 1906–1928 (2020).

86. P. H. Westfall, On using the bootstrap for multiple comparisons. *J. Biopharm. Stat.* **21**, 1187–1205 (2011).
87. M. Thulin, boot.pval: Bootstrap p-Values (2021); https://CRAN.R-project.org/package=boot.pval.
88. J. P. Mugler, J. R. Brookeman, Three-dimensional magnetization-prepared rapid gradient-echo imaging (3D MP RAGE). *Magn. Reson. Med.* **15**, 152–157 (1990).
89. O. Esteban, C. J. Markiewicz, M. Goncalves, E. DuPre, J. D. Kent, T. Salo, R. Ciric, B. Pinsard, R. W. Blair, R. A. Poldrack, K. J. Gorgolewski, fMRIPrep: A robust preprocessing pipeline for functional MRI. doi:10.5281/zenodo.4055773 (2020).
90. O. Esteban, C. J. Markiewicz, R. W. Blair, C. A. Moodie, A. I. Isik, A. Erramuzpe, J. D. Kent, M. Goncalves, E. DuPre, M. Snyder, H. Oya, S. S. Ghosh, J. Wright, J. Durnez, R. A. Poldrack, K. J. Gorgolewski, fMRIPrep: A robust preprocessing pipeline for functional MRI. *Nat. Methods* **16**, 111–116 (2019).
91. K. J. Gorgolewski, C. D. Burns, C. Madison, D. Clark, Y. O. Halchenko, M. L. Waskom, S. S. Ghosh, Nipype: A flexible, lightweight and extensible neuroimaging data processing framework in python. *Front. Neuroinform.* **5**, (2011).
92. O. Esteban, C. J. Markiewicz, D. Jarecka, E. Ziegler, H. Johnson, C. Burns, A. Manhães-Savio, C. Hamalainen, M. P. Notter, B. Yvernault, D. G. Ellis, T. Salo, M. Goncalves, K. Jordan, M. Waskom, J. Wong, E. Benderoff, D. Clark, F. Loney, B. E. Dewey, D. M. Nielson, C. Madison, S. Bougacha, R. Ćirić, M. G. Clark, M. Modat, M. Dayan, D. Clark, A. Keshavan, M. Visconti di Oleggio Castello, B. Pinsard, A. Gramfort, Y. O. Halchenko, H. Christian, S. Berleant, M. Joseph, J. Guillon, A. Rokem, S. Koudoro, R. Markello, E. DuPre, J. Kaczmarzyk, B. Moloney, B. Cipollini, G. Varoquaux, D. Wassermann, M. Hanke, G. de Hollander, D. Mordom, A. Gillman, C. Buchanan, A. Tabas, R. Tungaraza, W. M. Pauli, S. Sikka, J. Forbes, M. Mancini, S. Iqbal, Y. Schwartz, A. Richie-Halford, I. B. Malone, M. Dubois, C. Frohlich, D. Welch, K. Bottenhorn, A. Watanabe, J. M. Huntenburg, C. Cumba, B. N. Nichols, A. De La Vega, A. Eshaghi, A. S. Heinsfeld, D. Ginsburg, A. Schaefer, E. Kastman, B. Acland, F. Liem, J. Kent, J. Kleesiek, J. A. Lee, D. Erickson, S. Giavasis, C. Correa, A. Ghayoor, R. Küttner, M. F. Perez-Guevara, J. Millman, J. Lai, D. Zhou, R. Blair, C. Haselgrove, S. Tilley II, M. Renfro, S. Liu, A. E. Kahn, L. M. Sisk, S. Kim, F. Pérez-García, W. Triplett, L. Lampe, X.-Z. Kong, M. Hallquist, A. Chetverikov, M. Grignard, F. Ma, M. Cieslak, K. Chawla, J. Salvatore, A. Park, T. Glatard, R. Poldrack, R. C. Craddock, O. Hinds, M. Bilgel, K. Leinweber, S. Inati, L. N. Perkins, L. Snoek, L. Weninger, G. Cooper, A. Mattfeld, K. Matsubara, M. Noel, J. WEN, J. Stadler, B. Cheung, S. Urchs, O. Stanley, J. Durnez, E. Condamine, D. Geisler, A. Floren, S. Gerhard, M. Molina-Romero, D. Haehn, A. Weinstein, A. Tambini, W. Broderick, S. Rothmei, S. K. Andberg, R. Khanuja, K. Schlamp, J. Arias, D. Papadopoulos Orfanos, C. Tarbert, R. Harms, P. Sharp, M. R. Crusoe, M. Brett, M. Falkiewicz, K. Podranski, J. Linkersdörfer, G. Flandin, G. Lerma-Usabiaga, E. Ort, D. Shachnev, D. McNamee, B. Meyers, A. Van, A. Davison, D. Bielievtsov, C. J. Steele, L. Huang, I. Gonzalez, J. Warner, D. S. Margulies, O. Contier, A. Marina, V. Saase, T. Nickson, J. Varada, I. Schwabacher, J. Pellman, R. Khanuja, N. Pannetier, C. McDermottroe, P. G. Mihai, J. Lai, K. J. Gorgolewski, S. Ghosh, nipy/nipype: 1.3.0-rc1 (2019), doi:10.5281/ZENODO.3476537.
93. Y. Behzadi, K. Restom, J. Liau, T. T. Liu, A component based noise correction method (CompCor) for BOLD and perfusion based fMRI. *Hum. Brain Mapp.* **37**, 90–101 (2007).
94. L. Chang, Sam, E. Jolly, J. H. Cheong, A. Burnashev, A. Chen, S. Frey, cosanlab/nltools: 0.3.14 (2019), doi:10.5281/ZENODO.3251172.
95. K. J. Friston, S. Williams, R. Howard, R. S. J. Frackowiak, R. Turner, Movement-related effects in fMRI time-series. *Magn. Reson. Med.* **35**, 346–355 (1996).
96. F. Carota, N. Kriegeskorte, H. Nili, F. Pulvermüller, Representational similarity mapping of distributional semantics in left inferior frontal, middle temporal, and motor cortex. *Cereb. Cortex* **27**, 294–309 (2017).
97. B. J. Devereux, A. Clarke, A. Marouchos, L. K. Tyler, Representational similarity analysis reveals commonalities and differences in the semantic processing of words and objects. *J. Neurosci.* **33**, 18906–18916 (2013).
98. A. G. Liuzzi, A. Aglinskas, S. L. Fairhall, General and feature-based semantic representations in the semantic network. *Sci. Rep.* **10**, 8931 (2020).
99. N. Tzourio-Mazoyer, B. Landeau, D. Papathanassiou, F. Crivello, O. Etard, B. Delcroix, B. Mazoyer, M. Joliot, Automated anatomical labeling of activations in SPM using a macroscopic anatomical parcellation of the MNI MRI single-subject brain. *Neuroimage* **15**, 273–289 (2002).
100. J. A. Maldjian, P. J. Laurienti, J. H. Burdette, Precentral gyrus discrepancy in electronic versions of the Talairach atlas. *Neuroimage* **21**, 450–455 (2004).
101. J. A. Maldjian, P. J. Laurienti, R. A. Kraft, J. H. Burdette, An automated method for neuroanatomic and cytoarchitectonic atlas-based interrogation of fMRI data sets. *Neuroimage* **19**, 1233–1239 (2003).
102. H. Nili, C. Wingfield, A. Walther, L. Su, W. Marslen-Wilson, N. Kriegeskorte, A toolbox for representational similarity analysis. *PLOS Comput. Biol.* **10**, e1003553 (2014).
103. P. J. Rousseeuw, Silhouettes: A graphical aid to the interpretation and validation of cluster analysis. *J. Comput. Appl. Math.* **20**, 53–65 (1987).
104. J. Millman, Convolving with the hemodyamic response function (2015); www.jarrodmillman.com/rcsds/lectures/convolution_background.html.
105. R. Moseley, F. Carota, O. Hauk, B. Mohr, F. Pulvermüller, A role for the motor system in binding abstract emotional meaning. *Cereb. Cortex* **22**, 1634–1647 (2012).
106. R. J. Feise, Do multiple outcome measures require p-value adjustment? *BMC Med. Res. Methodol.* **2**, 8 (2002).
107. R. A. Armstrong, When to use the Bonferroni correction. *Ophthalmic. Physiol. Opt.* **34**, 502–508 (2014).
108. N. J. Tustison, B. B. Avants, P. A. Cook, Y. Zheng, A. Egan, P. A. Yushkevich, J. C. Gee, N4ITK: Improved N3 bias correction. *IEEE Trans. Med. Imaging* **29**, 1310–1320 (2010).
109. B. B. Avants, C. L. Epstein, M. Grossman, J. C. Gee, Symmetric diffeomorphic image registration with cross-correlation: Evaluating automated labeling of elderly and neurodegenerative brain. *Med. Image Annal.* **12**, 26–41 (2008).
110. Y. Zhang, M. Brady, S. Smith, Segmentation of brain MR images through a hidden Markov random field model and the expectation-maximization algorithm. *IEEE Trans. Med. Imaging* **20**, 45–57 (2001).
111. V. Fonov, A. C. Evans, K. Botteron, C. R. Almli, R. C. McKinstry, D. L. Collins; Brain Development Cooperative Group, Unbiased average age-appropriate atlases for pediatric studies. *Neuroimage* **54**, 313–327 (2011).
112. M. Jenkinson, S. Smith, A global optimisation method for robust affine registration of brain images. *Med. Image Anal.* **5**, 143–156 (2001).
113. D. N. Greve, B. Fischl, Accurate and robust brain image alignment using boundary-based registration. *Neuroimage* **48**, 63–72 (2009).
114. M. Jenkinson, P. Bannister, M. Brady, S. Smith, Improved optimization for the robust and accurate linear registration and motion correction of brain images. *Neuroimage* **17**, 825–841 (2002).
115. R. W. Cox, J. S. Hyde, Software tools for analysis and visualization of fMRI data. *NMR Biomed.* **10**, 171–178 (1997).
116. J. D. Power, A. Mitra, T. O. Laumann, A. Z. Snyder, B. L. Schlaggar, S. E. Petersen, Methods to detect, characterize, and remove motion artifact in resting state fMRI. *Neuroimage* **84**, 320–341 (2014).
117. T. D. Satterthwaite, M. A. Elliot, R. T. Gerraty, R. Kosha, J. Loughead, M. E. Calkins, S. B. Eickhoff, H. Hakonarson, R. C. Gur, R. E. Gur, D. H. Wolf, An improved framework for confound regression and filtering for control of motion artifact in the preprocessing of resting-state functional connectivity data. *Neuroimage* **64**, 240–256 (2013).
118. C. Lanczos, Evaluation of noisy data. *SIAM J. Numer. Anal.* **1**, 76–85 (1964).

Acknowledgments

Funding: This work was supported by the Brown University Office of the Vice President for Research Seed Fund Award GR300152 to O.F. **Author contributions:** D.d.B., J.M.v.B., and O.F. designed the research, with input from P.L.R. J.M.v.B. collected the data. D.d.B. conducted the analyses. D.d.B., J.M.v.B., and O.F. wrote the manuscript and P.L.R. provided edits. **Competing interests:** The authors declare that they have no competing interests. **Data and materials availability:** All data needed to evaluate the conclusions in the paper are present in the paper and/or the Supplementary Materials. The raw data will be provided by O.F. in compliance with Brown University's data transfer policy. Requests for the data should be submitted to oriel.feldmanhall@brown.edu.

Submitted 19 April 2022
Accepted 3 January 2023
Published 1 February 2023
10.1126/sciadv.abq5920